基の性質を示した。RNaseH 阻害活性を持つためには、(1)先ず活性中心にある Mg^{2+} イオンとキレートするような形で結合することが有効と推察された。化合物の中央には２つのカルボニル基が適当な間隔を空けて向きを変えて結合している。これが Mg^{2+} イオンにキレートすると期待される。チオフェンも Mg^{2+} イオンへのキレートを補助する役目を持ち、これまでスクリーニングで得られた化合物の多くが、この基本骨格を持っている。(2)チオフェンには硫酸基がついている。これは水溶性を上げる効果と RNaseH 側のアミノ酸と水素結合を形成する役目をもっている。特に標的と水素結合を形成して結合を安定化させると期待できる。(3)チオフェンと反対側には、疎水相互作用をするための２つのベンゼン環が配置され、結合部位を十分に適切に埋めるために、適当な間隔が必要であり、このためにジアゾ基が導入されている。(4)中央の窒素原子からは適当な大きさの官能基が結合していることが望ましく、このために水溶性も考慮してシアノ基を結合させている。

設計した化合物は、既存の認可薬との共通の構造を持たせることにも配慮している。これは合成の実績がある構造であることと、副作用の出にくい構造であることを担保するためである。図１０に示すように中央のペプチド結合は、プロテアーゼ阻害剤に良く見られる構造であり、例えば初期の HIV-1 プロテアーゼ阻害剤のリトナビルには、ペプチド結合が含まれている。末端の硫酸基はタウリンの主用骨格である。図１１に示すようにアゾベンゼンは、サラゾサルファピリジンに含まれている構造であり、サラゾサルファピリジンの主用骨格となっている。またシアノ基も、これを含む医薬品が実際に存在している。従って、既に認可された医薬品に使用されていることから、その部分構造が重篤な健康被害を生じる可能性が低くなっている。

E．結論

スクリーニング実験で得られた RNaseH に対する阻害活性を持つ薬物の構造をもとに、新規の化合物を考案した。考案した薬物について、RNaseH との結合構造をドッキングシミュレーションにより予測し、有望な化合物構造を選び出した。その一つについて、有機合成を試みた。また、その他の化合物について、委託合成などの方策を探っている。今後、幾つかの化合物の合成を達成し、これらの化合物について生化学実験により活性の評価を行っていく予定である。

F．研究発表

１．論文発表

- Ode, H., Matsuyama, S., Hata, M., Hoshino, T., Kakizawa, J., Sugiura, W. : Mechanism of Drug Resistance Due to N88S in CRF01_AE HIV-1 Protease Analyzed by Molecular Dynamics Simulations, J. Med. Chem. 50, 1768 - 1777 (2007)
- Ode, H., Matsuyama, S., Hata, M., Neya, S., Kakizawa, J., Sugiura, W., Hoshino, T.: Computational Characterization of Structural Role of the Non- active Site Mutation M36I of Human Immunodeficiency Virus Type 1 Protease, J. Mol. Biol. 370, 598-607 (2007)

２．総説

- 星野忠次，大出裕高: HIV プロテアーゼ阻害剤とウイルスの薬剤耐性、分子構造から考える薬物の作用機序(11)、医薬ジャーナル、Vol.43. No.12. pp.5-11 (2007)

3．学会発表

・ 大出裕高，松山　翔，畑　晶之，根矢三郎，杉浦　亙，星野忠次 「HIV-1 プロテアーゼ Non-active Site 変異 M36I の分子動力学的機能解析」日本薬学会第 127 年会要旨集-3，53（2007）富山
・ 高村　斉，大出裕高，新本裕子，根矢三郎，星野忠次 「新規抗 HIV 薬の合成研究」日本薬学会第 127 年会要旨集-3，54（2007）富山
・ 辰巳絢子，藤　秀義，高村　斉，駒野　淳，根矢三郎，星野忠次 「HIV-1 の RNaseH 活性を阻害する薬物の設計と評価」日本薬学会第 127 年会要旨集-3，54（2007）富山
・ 藤　秀義，辰巳絢子，栗田明宙，駒野　淳，星野忠次「コンピュータ支援による HIV-1 治療薬の開発」レトロウイルス研究会夏期セミナー2007 プログラム（2007）富士
・ 中里俊文，高村斉，大出裕高，清水愛，杉浦亙，星野忠次「L90M 変異体に阻害作用をもつ抗 HIV 薬の設計・合成」第 21 回日本エイズ学会学術集会・総会抄録集，167（2007）広島
・ 松山翔，大出裕高，柿澤淳子，杉浦亙，星野忠次「臨床検体由来 SubtypeC HIV-1 protease の薬剤耐性機構に関する構造化学的研究」第 21 回日本エイズ学会学術集会・総会抄録集，268（2007）広島
・ 柿澤淳子，松山翔，大出裕高，星野忠次，大高泰靖，岩谷靖雅，西澤雅子，Rajintha Bandaranayake，Celia A. Schiffer，杉浦亙「CRF01_AE とサブタイプ B のプロテアーゼの構造解析」第 21 回日本エイズ学会学術集会・総会抄録集，268（2007）広島
・ 大出裕高，横幕能行，松山翔，伊部史朗，藤崎誠一郎，間宮均人，濱口元洋，金田次弘，星野忠次「コンピュータ・シミュレーションで薬剤耐性 HIV-1 に対する薬効の予測は可能か?」第 21 回日本エイズ学会学術集会・総会抄録集，311（2007）広島
・ 藤秀義，浦野恵美子，厳　馬華，中原徹，堤浩，濱武牧子，宮内浩典，森川裕子，玉村啓和，杉浦亙，山本直樹，駒野淳，星野忠次「ドッキングシミュレーションによる HIV-1 インテグラーゼ阻害活性を有するペプチドの分子設計」第 45 回日本生物物理学会 講演予稿集，S126（2007）横浜

G．知的所有権の出願・取得状況（予定を含む）

実績無し。

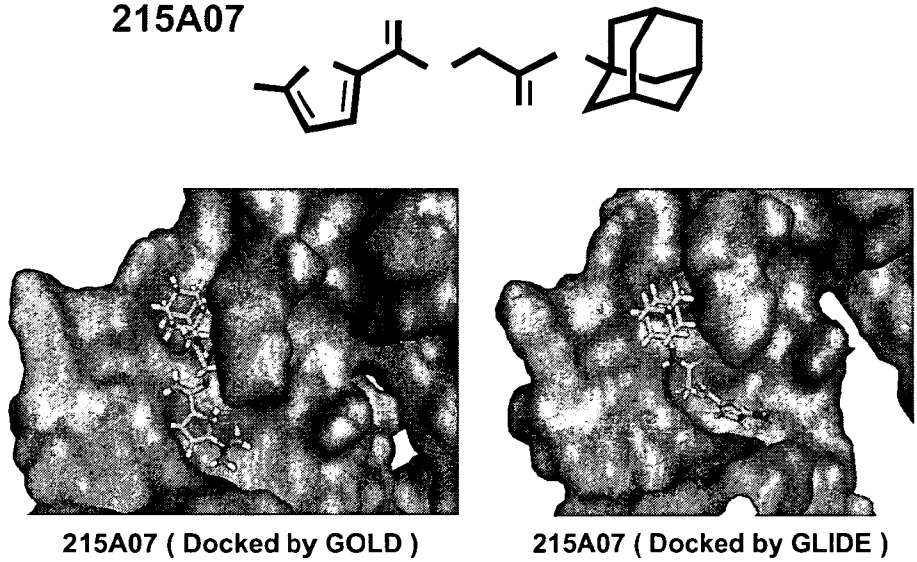

図１

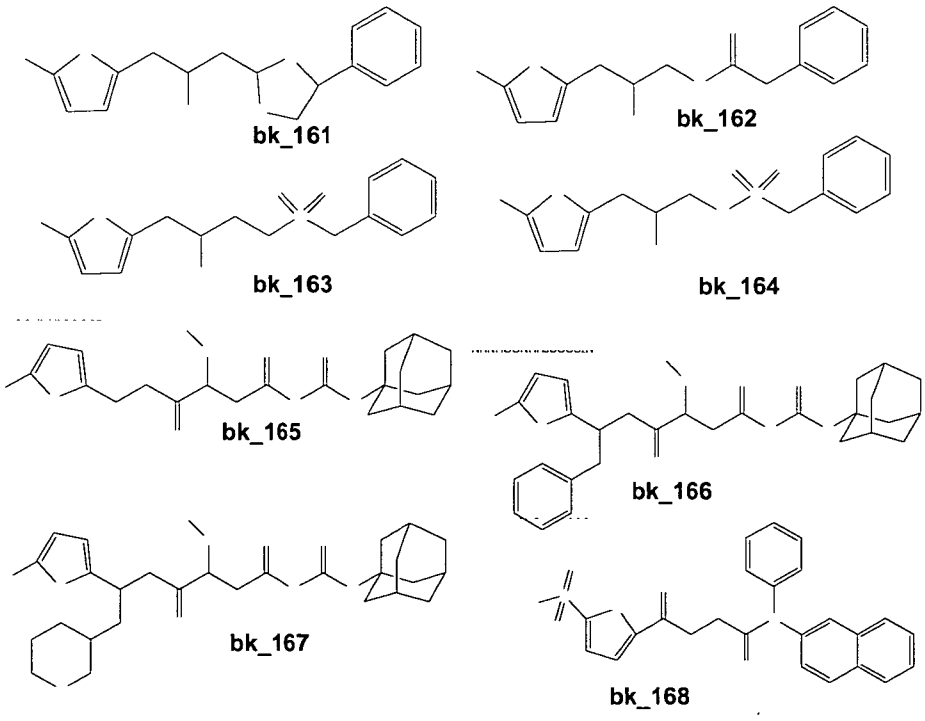

図２　*都合により一部意図的に図を消去するなど修正を施しています。

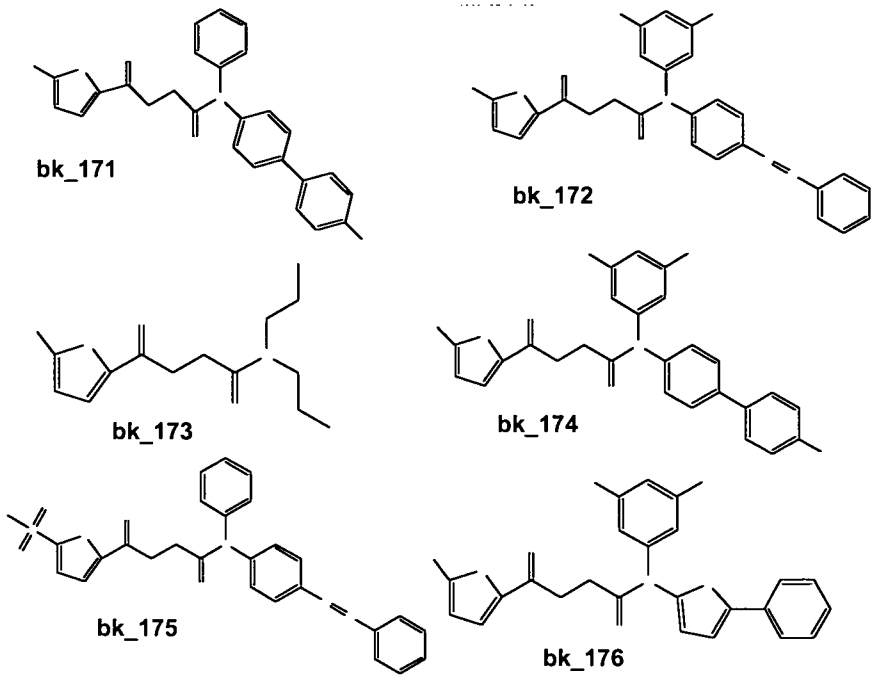

図３　*都合により一部意図的に図を消去するなど修正を施しています。

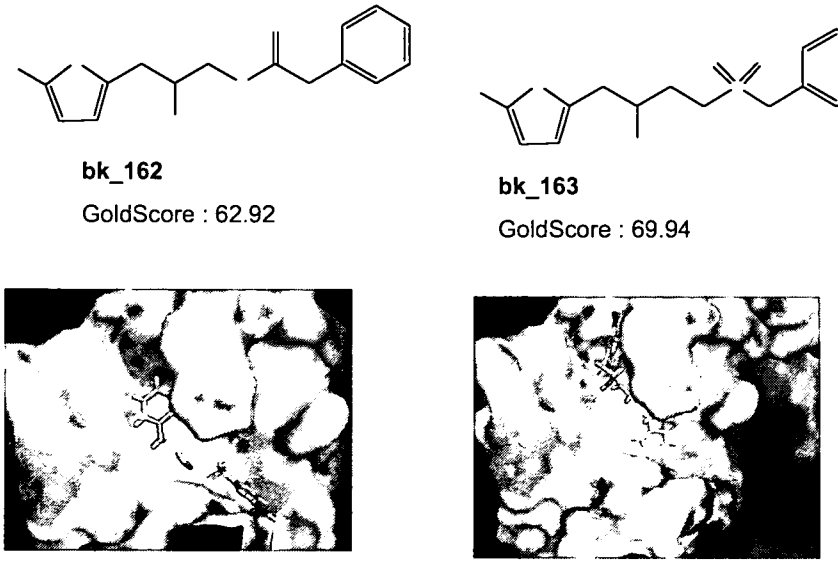

図４　*都合により一部意図的に図を消去するなど修正を施しています。

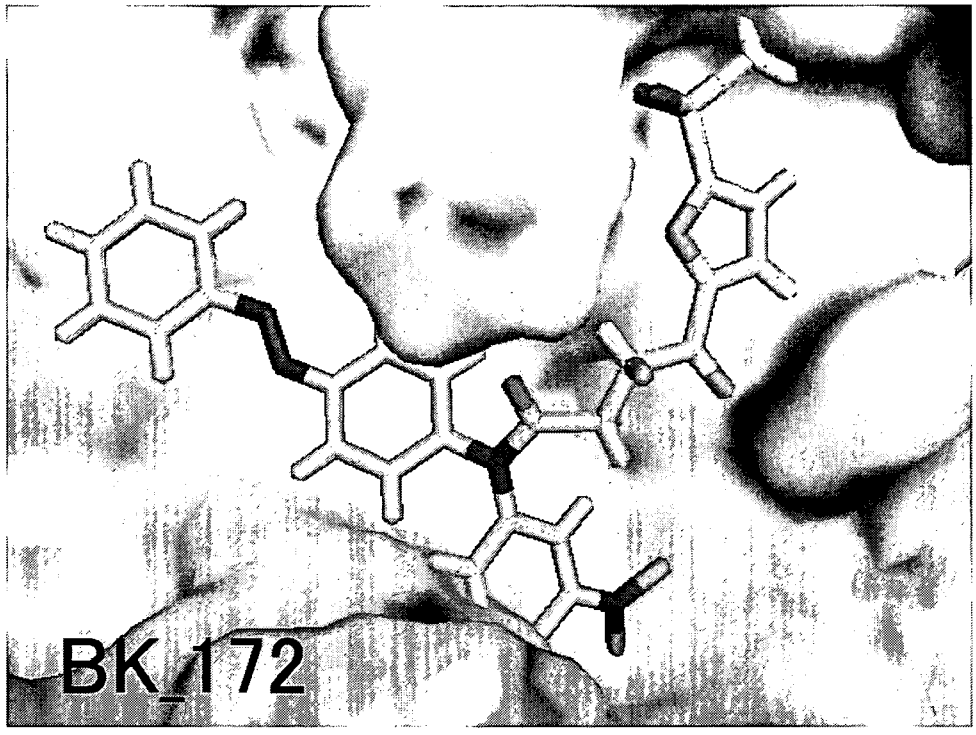

図５

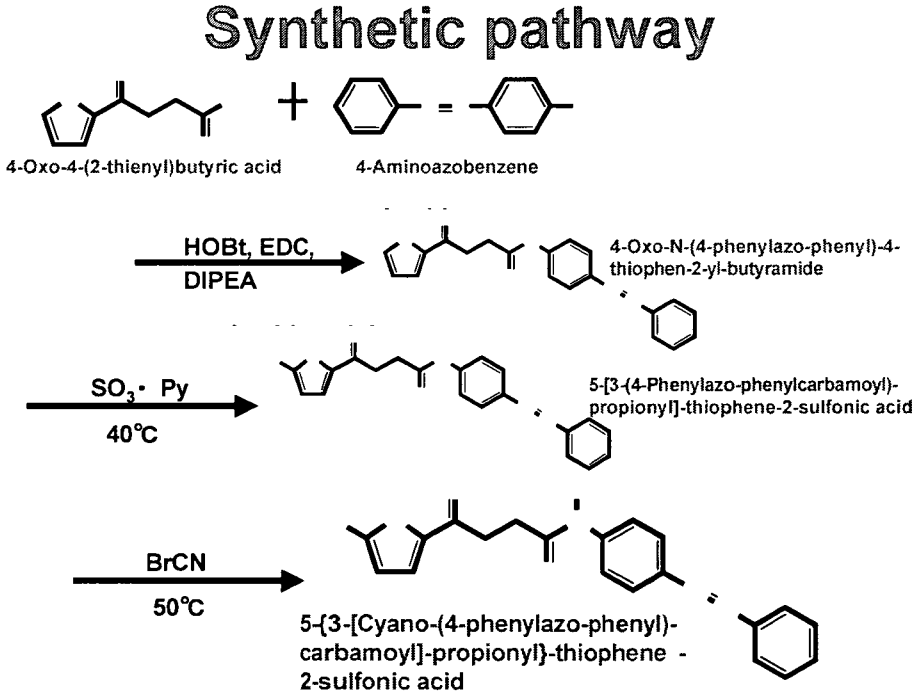

図６　*都合により一部意図的に図を消去するなど修正を施しています。

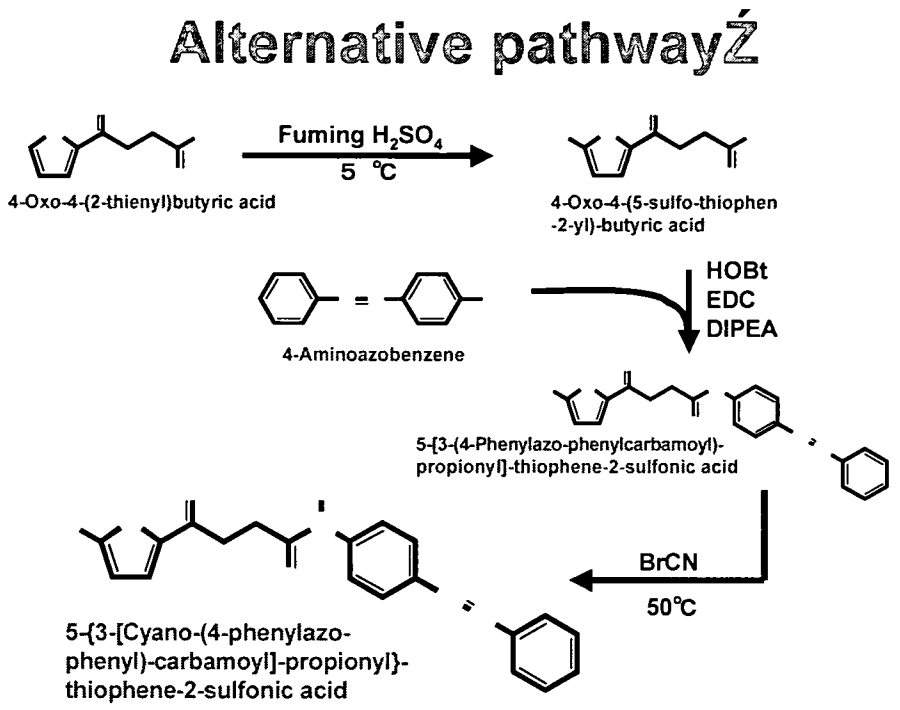

図７　*都合により一部意図的に図を消去するなど修正を施しています。

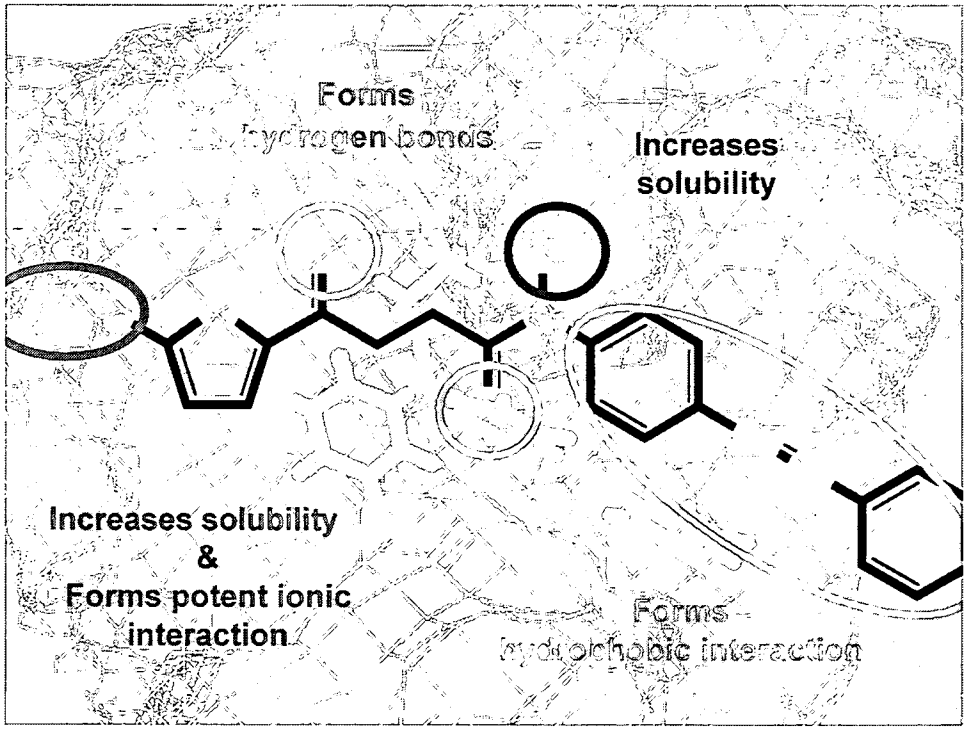

図８　*都合により一部意図的に図を消去するなど修正を施しています。

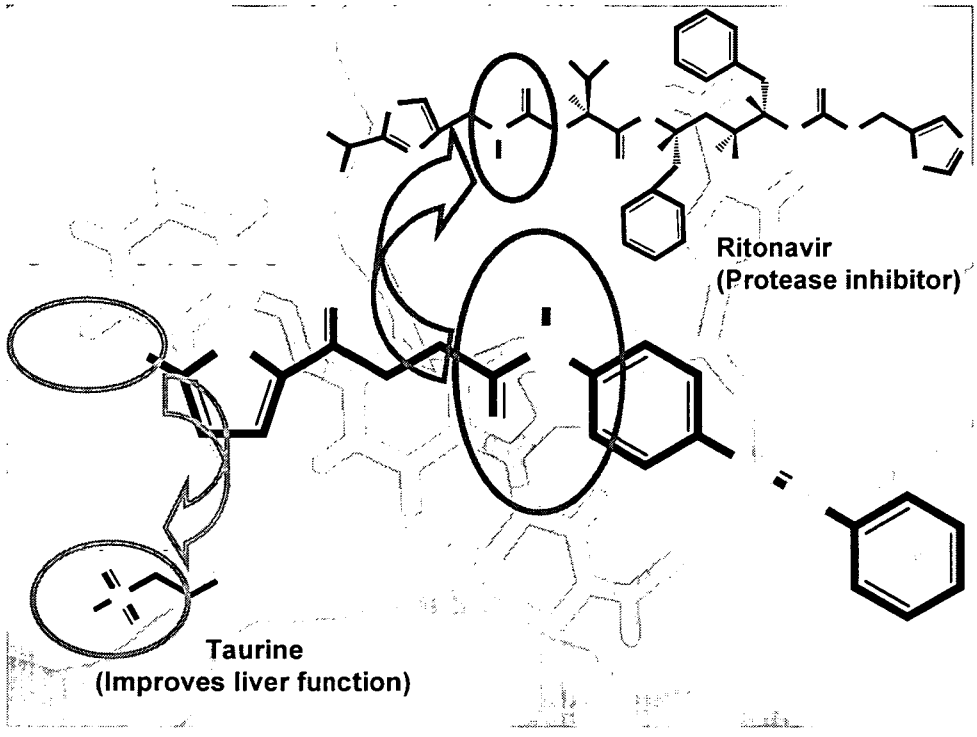

図９　*都合により一部意図的に図を消去するなど修正を施しています。

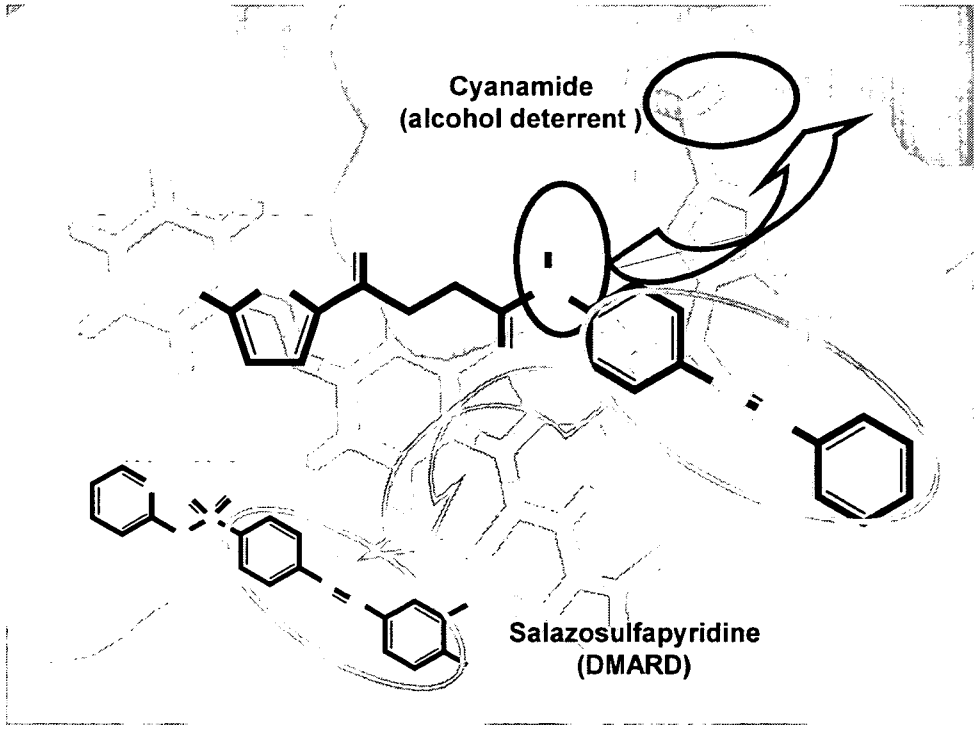

図１０　*都合により一部意図的に図を消去するなど修正を施しています。

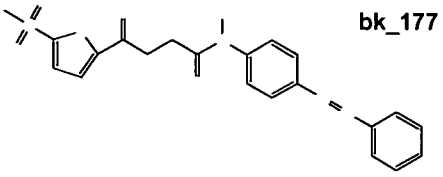

新規化合物構築から評価までの流れ

① 新規化合物の構築　(ChemDrawにてmol形式で保存)

② PRODRG Serverにてpdb形式へ変換

③ nfutilを用いて mol2形式に変換

④ GOLDを用いてドッキング

(タンパクの構造は以前使用したものと同じ　)

⑤ ドッキング結果より、活性部位に結合したもののうち

スコアの良いものを抽出

⑥　Orientationにてエネルギー算出・評価

図１１　*都合により一部意図的に図を消去するなど修正を施しています。

lll. 平成１９年度　業績一覧

研究成果の刊行に関する一覧表

主任研究者　駒野　淳

書籍:なし

雑誌

発表者氏名	論文タイトル	発表誌名	巻号	ページ	出版年
Emiko Urano, Saki Shimizu, Yuko Futahashi, Makiko Hamatake, Yuko Morikawa, Naoko Takahashi, Hidesuke Fukazawa, Naoki Yamamoto, Jun Komano.	Cyclin K/CPR4 inhibits primate lentiviral replication by inactivating Tat/P-TEFb-dependent LTR transcription.	*AIDS, In press*	-	-	2008
Akihide Ryo, Naomi Tsurutani, Kenji Ohba, Ryuichiro Kimura, Jun Komano, Mayuko Nishi, Hiromi Soeda, Shinichiro Hattori, Kilian Perrem, Mikio Yamamoto, Joh Chiba, Jun-ichi Mimaya, Kazuhisa Yoshimura, Shuzo Matsushita, Mitsuo Honda, Akihiko Yoshimura, Ichiro Aoki, Yuko Morikawa and Naoki Yamamoto.	SOCS1 is an inducible host factor during HIV-1 infection and regulates the intracellular trafficking and stability of HIV-1 Gag.	*PNAS, In press*	105(1)	294-299	2008
Takeshi Yoshida, Yuji Kawano, Kei Sato, Yoshiharu Miura, Yoshinori Ando, Jun Aoki, Jun Komano, Yuetsu Tanaka, Yoshio Koyanagi.	CD63 and its mutants disrupt CXCR4 trafficking to the plasma membrane and inhibit T-cell tropic HIV-1 entry.	*Traffic, In press*	-	-	2007
Matsuda Z, Iga M, Miyauchi K, Komano J, Morishita K, Okayama A, Tsubouchi H.	In vitro translation to study HIV protease activity.	*Methods Mol Biol.*	375	135-149	2007
Kameoka M, Kitagawa Y, Utachee P, Jinnopat P, Dhepakson P, Isarangkura-na-ayuthaya P, Tokunaga K, Sato H, Komano J, Yamamoto N, Oguchi S, Natori Y, Ikuta K.	Identification of the suppressive factors for human immunodeficiency virus type-1 replication using the siRNA mini-library directed against host cellular genes.	*Biochem Biophys Res Commun.*	359(3)	729-734.	2007
Futahashi Y, Komano J, Urano E, Aoki T, Hamatake M, Miyauchi K, Yoshida T, Koyanagi Y, Matsuda Z, Yamamoto N.	Separate elements are required for ligand-dependent and -independent internalization of metastatic potentiator	*Cancer Science.*	98(3)	373-379	2007

	CXCR4.				
Shimizu S, Urano E, Futahashi Y, Miyauchi K, Isogai M, Matsuda Z, Nohtomi K, Onogi T, Takebe Y, Yamamoto N, Komano J.	Inhibiting lentiviral replication by HEXIM1, a cellular negative regulator of the CDK9/cyclin T complex.	*AIDS*	21(5)	575-582	2007

和文

村上 努、駒野 淳.	ARV の Universal Access 時代を迎えて; エイズ研究センターの国際研修活動について	病原微生物検出情報	28(6)	164-166	2007
Murakami T, Gottlinger H, Morikawa Y, Komano J, Ryo A, Sato H.	Regulation of Gag trafficiking and functions (Review)	The Journal of AIDS Research	9(2)	102-107	2007

分担研究者　星野　忠治

書籍:なし

雑誌

発表者氏名	論文タイトル名	発表誌名	巻号	ページ	出版年
Takaoka, T., Mori, K., Okimoto, N., Neya, S., Hoshino, T.	Prediction of the structure of complexes comprised of proteins and glycosaminoglycans using docking simulation and cluster analysis	J. Chem. Theor. Comput.	3	2347-2356	2007
Ode, H., Matsuyama, S., Hata, M., Neya, S., Kakizawa, J., Sugiura, W., Hoshino, T.	Computational Characterization of Structural Role of the Non- active Site Mutation M36I of Human Immunodeficiency Virus Type 1 Protease	J.Mol. Biol	370	598-607	2007
Ode, H., Matsuyama, S., Hata, M., Hoshino, T., Kakizawa, J., Sugiura, W.	Mechanism of Drug Resistance Due to N88S in CRF01_AE HIV-1 Protease Analyzed by Molecular Dynamics Simulations	J. Med. Chem.	50	1768-1777	2007
Kanari, Y., Shoji, Y., Ode, H., Miyake, T., Tanii, T., Hoshino, T., Ohdomari, I.	Protein Adsorption on Self-Assembled Monolayers Induced by Surface Water Molecule	Jpn. J. Appl. Phys.	46	6303-6308	2007

IV. 平成１９年度　刊行物別刷（抜粋）

刊行物別刷解説

1. Mechanism of Drug Resistance Due to N88S in CRF01_AE HIV-1 Protease Analyzed by Molecular Dynamics Simulations (Ode et al.)

アジアで流行するウイルス株CRF01 AEにおけるprotease inhibitor NFVに対する薬剤耐性変異がどのような原因で生じてくるかを電算機プログラムを用いたシミュレーションで探った研究。

2. Computational Characterization of Structural Role of the Non-active Site Mutation M36I of Human Immunodeficiency Virus Type 1 Protease (Ode et al.)

電算機解析によりprotease inhibitorであるNFVがproteaseと結合した構造を計算し、酵素の活性中心と位置のずれた部分に生じるM36I変異が酵素—阻害剤結合に与える影響を考察したもの。

3. Inhibiting lentiviral replication by HEXIM1, a cellular negative regulator of the CDK9/cyclin T complex (Shimizu et al.)

宿主因子であるHEXIM1タンパク質の発現増強がHIV-1およびSIVの複製を抑制することを直接的に証明した研究。HIV-1複製の分子メカニズムを理解して宿主因子の中に新たな創薬標的をみつけだすための研究の一例。

4. Separate elements are required for ligand-dependent and -independent internalization of metastatic potentiator CXCR4 (Futahashi et al.)

ウイルスレセプターの一つであるCXCR4における細胞表面発現の制御について解析した研究で、ウイルスレセプターの発現を制御する事によりエイズ治療薬を開発しようとするアプローチの基礎的知見。

Mechanism of Drug Resistance Due to N88S in CRF01_AE HIV-1 Protease, Analyzed by Molecular Dynamics Simulations

Hirotaka Ode,*,† Shou Matsuyama,† Masayuki Hata,† Tyuji Hoshino,†,‡ Junko Kakizawa,§ and Wataru Sugiura§

Graduate School of Pharmaceutical Sciences, Chiba University, 1-33 Yayoi-cho, Inage-ku, Chiba 263-8522, Japan, PRESTO, JST, 4-1-8 Honcho, Kawaguchi, Saitama 332-0012, Japan, and AIDS Research Center, National Institute of Infectious Diseases, 4-7-1 Gakuen, Musashimurayama, Tokyo 208-1011, Japan

Received October 6, 2006

Nelfinavir (NFV) is a currently available HIV-1 protease (PR) inhibitor. Patients in whom NFV treatment has failed predominantly carry D30N mutants of HIV-1 PRs if they have been infected with the subtype B virus. In contrast, N88S mutants of HIV-1 PRs predominantly emerge in patients in whom NFV treatment has failed and who carry the CRF01_AE virus. Both D30N and N88S confer resistance against NFV. However, it remains unclear why the nonactive site mutation N88S confers resistance against NFV. In this study, we examined the resistance mechanism through computational simulations. The simulations suggested that despite the nonactive site mutation, N88S causes NFV resistance by reducing interactions between PR and NFV. We also investigated why the emergence rates of D30N and N88S differ between subtype B and CRF01_AE HIV-1. The simulations suggested that polymorphisms of CRF01_AE PR are involved in the emergence rate of the drug-resistant mutants.

Introduction

Human immunodeficiency virus type 1 (HIV-1) is one of the most hazardous viruses for humans, and there is still a risk of a worldwide HIV-1 pandemic. HIV-1 has high genetic variability and has been classified into three groups labeled M, N, and O. Viruses in group M are further divided into subtypes, subsubtypes, and circulating recombinant forms (CRFs). The subtype B virus is commonly found in HIV-1-infected patients in the Americas, Europe, and Japan. In contrast, developing countries suffer from a growing epidemic of nonsubtype B viruses.

HIV-1 proliferates with the assistance of its own aspartic protease, so-called HIV-1 protease (HIV-1 PR), in its life cycle.[1] HIV-1 PR is an enzyme composed of two identical polypeptides each consisting of 99 amino acid residues, and its function is to process the viral Gag and Gag-Pol polyprotein precursors (Figure 1A). Because this processing is essential for viral maturation, inhibition of PR function leads to incomplete viral replication and prevents the transfer to other cells.[2] Therefore, HIV-1 PR is an attractive target for anti-HIV-1 drugs. Nine PR inhibitors (PIs)[3−11] have been approved by the FDA and have successfully lowered the death rate due to acquired immune deficiency syndrome (AIDS) in advanced countries during the past decade. However, the currently available PIs were developed and tested only against subtype B PRs. Few studies have examined the susceptibility of nonsubtype B viruses to those PIs, and no standard protocol of chemotherapy for nonsubtype B viruses has been established.[12−17]

Recently, Ariyoshi et al. reported that the pattern of drug-resistant mutations differed between subtype B and CRF01_AE (subtype AE) HIV-1.[16] Mutations of L10F, K20I, L33I, and N88S in PR were more frequently seen in patients infected with subtype AE HIV-1 than in patients infected with subtype B HIV-1. Mutations of D30N, A71V, and N88D in PR were found in patients with subtype B HIV-1. Most of the charac-

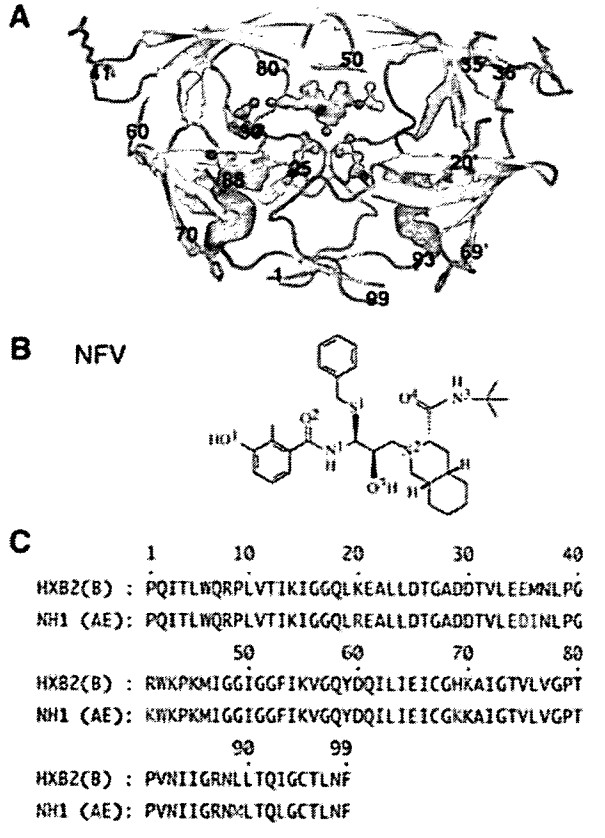

Figure 1. (A) Structure of HIV-1 PR. Locations of two catalytic aspartates, the 30th and the 88th residues, are shown in ball and stick representation. Locations of polymorphisms in subtype AE PR (K20R, E35D, M36I, R41K, H69K, L89M, and I93L) are shown in stick representation. (B) Chemical structure of NFV. (C) Amino acid sequences of a wild-type (WT) subtype B HIV-1 PR (HXB2) and a reference sequence of subtype AE HIV-1 PR (NH1). The polymorphisms in subtype AE PR are highlighted in red letters.

* To whom correspondence should be addressed. Phone: +81-43-290-2926. Fax: +81-43-290-2925. E-mail: odehir@graduate.chiba-u.jp.
† Chiba University.
‡ PRESTO.
§ National Institute of Infectious Diseases.

10.1021/jm061158i CCC: $37.00
Published on Web 03/17/2007

teristic mutation patterns in that study were associated with a history of treatment with nelfinavir (NFV, Figure 1B), an FDA-approved PI. D30N and N88S are particularly related to resistance against NFV.[18-21] Interestingly, N88S is also known to cause hypersensitivity to another PI, amprenavir. We have previously suggested by computational simulations that D30N in subtype B PR confers resistance against NFV by canceling hydrogen bonds between NFV and N30.[22] In addition, we and other groups have proposed an explanation of why some mutations confer resistance against PIs by not only X-ray crystallography[23-33] but also computational studies.[34-41] However, it has not been clarified why N88S in subtype AE PR confers resistance against NFV. Since N88S occurs at a nonactive site of PR, it is difficult to speculate on the mechanism of resistance. Furthermore, it has not been understood why N88S emerges more predominantly than D30N in patients with subtype AE HIV-1 or why D30N emerges more predominantly than N88S in patients with subtype B HIV-1. Subtype AE HIV-1 has natural polymorphisms, K20R, E35D, M36I, R41K, H69K, L89M, and I93L, in PR unlike subtype B HIV-1 (Figure 1C). These polymorphisms are also located at the nonactive site of PR. It is still uncertain whether or not the polymorphisms affect the emergence rates of those mutations.

In this study, we investigated the mechanism of resistance against NFV due to N88S in subtype AE HIV-1 PR through computational simulations. Our simulations indicated that the N88S mutation creates hydrogen bonds between the D30 and S88 side chains. Therefore, N88S mutation reduces interactions between D30 and NFV. We also investigated the reason for the difference between the two subtypes in the emergence rate of D30N as well as that of N88S. The results indicated that, in subtype B HIV-1, D30N PR has a lower affinity for NFV than does N88S PR. In subtype AE HIV-1, on the other hand, D30N PR has a higher affinity than does N88S. Our findings suggest that despite the nonactive site mutations, the polymorphisms regulate the emergence rates of these drug-resistant mutants.

Results

Reconsideration of Torsional Force Field Parameters for Benzamide. Before carrying out molecular dynamics (MD) simulations, we reconsidered torsional force field parameters for benzamide: CA−CA−C−N and CA−CA−C−O (Supporting Information Figure S1). The benzamide group comprises a part of NFV. The benzamide moiety in NFV has an important interaction with D30 of PR.[22,42] Nevertheless, the AMBER ff03[43] and general AMBER force fields[44] cause a much higher energy barrier around the rotatable bond between the benzene and amide groups in benzamide than that based on quantum chemical calculations. This is a serious problem for our simulations. The force field parameters for benzamide need to be carefully examined and preferably changed from the original AMBER force fields, as described in the AMBER Archive in 2003.[45] Since these force field parameters have not been changed in the AMBER force fields yet, we improved the torsional force field parameters for the benzamide moiety in NFV. The torsional parameters were generated in the same manner as that for the development of the AMBER ff03 force field. The obtained parameters are listed in Table 1. We executed MD simulations using these newly developed force field parameters.

Hydrogen Bonds between NFV and PRs. Hydrogen bonds play an important role in protein−ligand bindings. First, we examined the hydrogen bonds between NFV and PR in each complex: wild-type (WT) PR, D30N PR, and N88S PR of subtype B HIV-1 (labeled B(WT), B(D30N), and B(N88S), respectively); the reference (Ref) PR, D30N PR, and N88S PR of subtype AE HIV-1 in complex with NFV (AE(Ref), AE(D30N), and AE(N88S)). We examined 1000 snapshot structures for the last 1.0 ns and identified direct or one-water-molecule-mediated hydrogen bonds (Table 2 and Supporting Information Table S1 and Figure S2). All six PRs create similar hydrogen bond networks. The side chains of both D25 and D25′ interact with the central hydroxyl group of NFV (the atom corresponding to O3 in Figure 1B). One water molecule mediates the interaction between the main chains of I50/I50′ and NFV. Furthermore, another water molecule mediates the interaction between D29′ and NFV. However, the interaction between NFV and the 30th residue has variations among the six PRs. In B(WT) and AE(Ref), either the main chain or the side chain of D30 makes a direct hydrogen bond with NFV. D30N and N88S models show different interactions between subtype B and AE PRs. B(D30N) has no hydrogen bond between N30 and NFV, whereas AE(D30N) has direct or one-water-molecule-mediated hydrogen bonds. B(N88S) frequently creates a direct hydrogen bond between the main chain of D30 and NFV. On the other hand, AE(N88S) mainly creates one-water-molecule-mediated hydrogen bonds between the main chain of D30 and NFV. Interestingly, the side chain of N30 in AE(D30N) is clearly closer to the phenol group of NFV than that of B(D30N) (Figure 2). In contrast, the side chain of D30 in AE(N88S) is more distant from the phenol group of NFV than that of B(N88S).

Table 1. Force Field Parameters for the Torsional Parameters of the Benzamide Part of NFV[a]

CA−CA−C−N			CA−CA−C−O		
$V_n/2$	n	γ	$V_n/2$	n	γ
Developed Parameters					
0.90	2	180.0	0.90	2	180.0
0.05	4	0.0	0.05	4	0.0
AMBER ff03 Force Field					
3.63	2	180.0	3.63	2	180.0

[a] Torsional energy is given by $E = (V_n/2)[1 + \cos(n\phi - \gamma)]$.

Hydrogen Bonds of the Side Chain of the 30th Residue with PR Residues. In B(D30N) and in AE(N88S), the side chain of the 30th residue does not create any hydrogen bonds with NFV. To clarify the effects of the D30N and N88S mutations in detail, the interactions of the side chain of the 30th residue with other residues of PR were investigated as shown in Table 3. B(WT) and AE(Ref) have an interaction between the side chains of D30 and K45. B(D30N) has direct hydrogen bonds from the side chain of N30 to T31 and T74. On the other hand, AE(D30N) has one-water-molecule-mediated hydrogen bonds from N30 to T31, T74, and N88. T31, T74, and N88 also create hydrogen bond networks at the nonactive sites in B(WT) and AE(Ref), although D30 is not involved in the networks (Supporting Information Table S2). The side chains of D30 in both B(N88S) and AE(N88S) have either a direct hydrogen bond with the side chain of S88 or one-water-molecule-mediated hydrogen bonds with T31, T74, and S88. The mutations D30N and N88S affect those hydrogen bond networks.

Comparison of the Structures with B(WT). To clarify the effects of mutations at the 30th and the 88th residues on the active site conformations, the average structure of each model for the last 1.0 ns was compared with that of B(WT). Each model was fitted to B(WT) using the coordinates of main chain atoms N, Cα, and C, and the root mean squared deviation (rmsd) value was calculated (Figure 3). When the active site residues of each PR are compared with those of B(WT), conformational

Table 2. Hydrogen Bond Networks of NFV with D30 or N30 in PR

subtype B					subtype AE				
donor		acceptor		%[a]	donor		acceptor		%
		B(WT)					AE(ref)		
N	D30	O1[b]	NFV	30.7	N	D30	O1	NFV	5.7
O1	NFV	OD1/OD2	D30	31.6	O1	NFV	OD1/OD2	D30	69.2
O1	NFV	O	D30	42.9	O1	NFV	O	D30	9.0
		B(D30N)					AE(D30N)		
					O1	NFV	OD1	N30	25.2
					O1	NFV	O	WAT766	12.6
					O	WAT766	OD1	N30	12.1
					O1	NFV	O	WAT1770	8.4
					O	WAT1770	OD1	N30	6.8
					O1	NFV	O	WAT8063	13.7
					O	WAT8063	OD1	N30	9.1
		B(N88S)					AE(N88S)		
N	D30	O1	NFV	26.7	N	D30	O1	NFV	7.4
O1	NFV	OD2	D30	12.4	O1	NFV	O	D30	27.9
O1	NFV	O	D30	56.7	O1	NFV	O	WAT6715	28.8
					N	D30	O	WAT6715	28.3
					O	WAT6715	N	D30	12.6
					O	WAT6715	O	D30	31.8
					O1	NFV	O	WAT7886	13.6
					O	WAT6715	OD1	D30	5.2
					O	WAT6715	O	D30	25.5

[a] Occupancy of hydrogen bonds during 2.0−3.0 ns of MD simulation. [b] The atom names of NFV are shown in Figure 1.

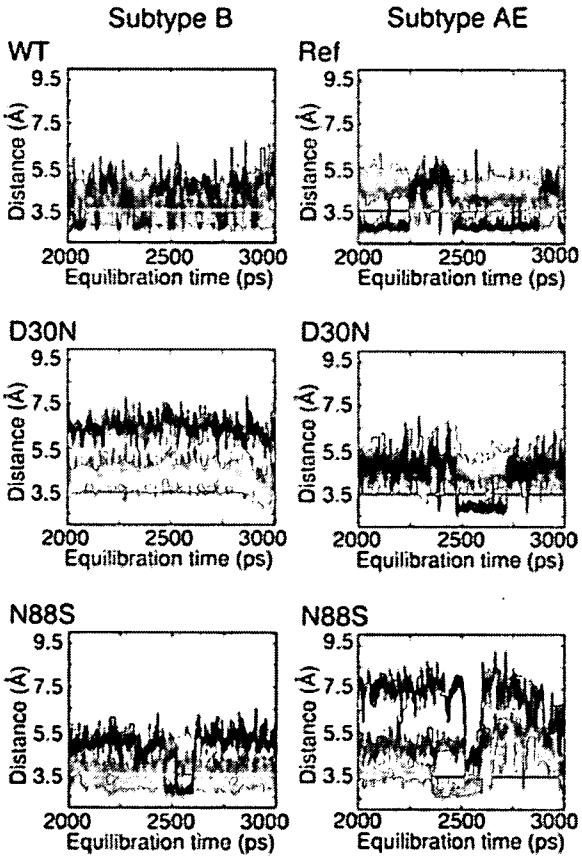

Figure 2. Distance between NFV and the 30th residue. Each red and green solid line corresponds to the distance between N of the 30th residue and the O1 atom of NFV and to the distance between O of the 30th residue and the O1 atom of NFV. Blue solid lines of B(WT), AE(Ref), B(N88S), and AE(N88S) show the distances between O1 of NFV and OD1/OD2 of D30, while those of B(D30N) and AE(D30N) show the distances between O1 of NFV and OD1/ND2 of N30.

changes are observed only on the active site residues around the 30th residue. AE(N88S) shows a large conformational change at D30 (rmsd = 1.5 ± 0.4 Å, Figure 4). The other four models (B(D30N), B(N88S), AE(Ref), and AE(D30N)) show a slight conformational change at D30. When each subtype B PR is compared with the corresponding subtype AE PR, B(D30N) is found to have larger conformational changes on N30 than AE(D30N). AE(N88S) shows larger conformational changes on D30 than B(N88S). Next, we compared the location of NFV in each model with that of B(WT). The benzamide group of NFV, which interacts with the 30th residue, shows a larger positional deviation than do other parts of NFV in every model (Supporting Information Figure S3).

Binding Free Energy Calculations. The influence of mutation or polymorphism on the binding free energy ΔG_b was examined for each model. Table 4 shows the results of MM/PBSA calculations for all of the PRs in complex with NFV. In subtype B HIV-1, B(D30N) reduces the binding energy with NFV from B(WT) more than B(N88S) does. On the other hand, in subtype AE HIV-1, AE(D30N) shows affinity with NFV, similar to AE(Ref), and has a higher affinity with NFV than AE(N88S). The results correspond to the emergence rates of subtypes B and AE variants in patients in whom NFV treatment has failed. D30N predominantly emerges in patients with subtype B HIV-1, whereas N88S predominantly emerges in patients with subtype AE HIV-1. We also investigated the contributions of the respective residues to binding free energy (Figure 5). In all six models, the active site residues stabilize the complex of each PR and NFV. When we focus on the binding energy due to the 30th residue, D30 or N30, B(D30N) reduces the contribution to the binding free energy in comparison with B(WT) (Figure 6). AE(N88S) also reduces the contribution to the binding energy compared with AE(Ref). B(N88S) shows a contribution similar to that of B(WT), and AE(D30N) shows a contribution similar to that of AE(Ref).

Discussion

In this study, we performed MD simulations of HIV-1 PRs in complex with NFV for the purpose of clarifying (1) the mechanism of resistance against NFV due to N88S in subtype

Table 3. Hydrogen Bond Networks of the Side Chain of D30 or N30 with PR Residues

subtype B					subtype AE				
donor		acceptor		%[a]	donor		acceptor		%
		B(WT)					AE(Ref)		
NZ	K45	OD1/OD2	D30	67.0	NZ	K45	OD1	D30	38.3
		B(D30N)					AE(D30N)		
ND2	N30	O	T74	89.7	ND2	N30	O	WAT224	76.9
ND2	N30	N	T31	59.5	N	T31	O	WAT224	72.6
ND2	N30	O	T31	98.1	O	WAT224	O	T31	70.7
N	T31	ND2	N30	67.9	O	WAT224	O	T74	76.8
					ND2	N88	O	WAT224	39.4
		B(N88S)					AE(N88S)		
OG	S88	OD1	D30	34.7	OG	S88	OD2	D30	77.8
O	WAT1142	OD1/OD2	D30	46.2	O	WAT226	OD2	D30	33.7
N	T31	O	WAT1142	38.3	OG1	T31	O	WAT226	18.1
O	WAT1142	O	T74	45.1	N	T31	O	WAT226	31.4
OG	S88	O	WAT1142	40.9	O	WAT226	O	T74	33.8

[a] Occupancy of hydrogen bonds during 2.0–3.0 ns of MD simulation.

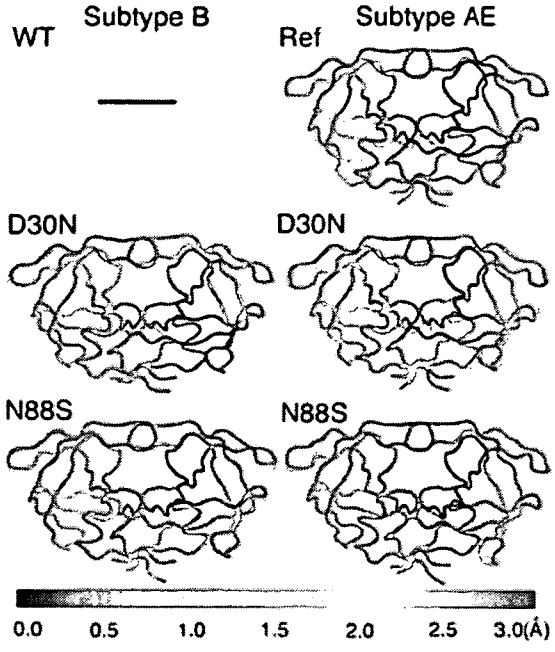

Figure 3. A 3D plot of rmsd of the average structure of each model from that of B(WT). The PR in each model is shown in colored tube representation. The color refers to the magnitude of rmsd shown in the bottom bar. Each model was fitted to B(WT) using the coordinates of main chain atoms N, Cα, and C of PR. The superimposed gray sticks and tubes represent the structure of B(WT).

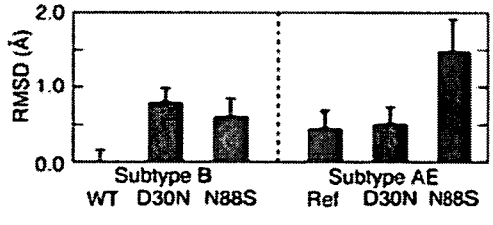

Figure 4. The rmsd value on the 30th residue of the average structure of each PR from that of B(WT). Error bars show root-mean-squared fluctuations (rmsf).

AE PR and (2) the reason that the emergence rates of D30N and N88S differ between subtypes B and AE HIV-1.

The 88th residue is located at a nonactive site of HIV-1PR. Thus, it is difficult to speculate on the mechanism of resistance due to N88S. Our simulations indicate that N88S mutant PR has a lower affinity with NFV than does Ref PR in subtype AE HIV-1, owing to the following mechanism. First, a hydrogen bond between the side chain of D30 and the side chain of S88 is created (Figure 7). Second, the location of D30 is changed. Finally, the interaction between D30 and NFV is reduced. N88S indirectly affects the binding between NFV and D30. Accordingly, both N88S and D30N are thought to confer specific resistance against NFV because the interaction with D30 is an essential factor for NFV binding. Indeed, it has been reported that the emergence of the N88S mutation is highly related to resistance against NFV.[18–21] N88D is another frequently observed mutation at the 88th residue of PR. It has also been reported that N88D changes the interactions of the 88th residue with D30, T31, and T74.[22,26] However, N88D hardly affects the ligand binding at the active site and does not cause resistance against NFV. N88S changes the interactions in a manner different from that of N88D.

We then pose another question: Why does N88S emerge more frequently in patients with subtype AE HIV-1 in whom NFV treatment has failed than in patients with subtype B HIV-1? Ariyoshi et al. reported that D30N emerged predominantly in patients with subtype B HIV-1 whereas N88S appeared predominantly in patients with subtype AE HIV-1.[16] Subtype AE HIV-1 PR has some natural polymorphisms (K20R, E35D, M36I, R41K, H69K, L89M, and I93L) unlike subtype B PR. These amino acids are located at nonactive sites of PR. To reveal whether the polymorphisms affect NFV binding or what causes the difference in the emergence rates of D30N and N88S, we carried out simulations of NFV complexes of WT PR, D30N PR, and N88S PR of subtype B (B(WT), B(D30N), B(N88S)) and Ref PR, D30N PR, and N88S PR of subtype AE (AE(Ref), AE(D30N), AE(N88S)). AE(Ref) has an interaction with NFV similar to that of B(WT). On the other hand, D30N and N88S mutations show different effects between subtypes B and AE PRs. D30N in subtype B PR greatly reduces the binding affinity with NFV because the hydrogen bonds between N30 and NFV are canceled, as we previously reported.[22] In contrast, D30N in subtype AE PR hardly affects the affinity with NFV. AE(D30N) has direct or one-water-molecule-mediated hydrogen bonds between N30 and NFV. On the other hand, N88S in subtype AE PR significantly reduces the binding affinity with NFV, whereas N88S in subtype B PR hardly affects the affinity with NFV. In both B(N88S) and AE(N88S), a hydrogen bond is created between the side chain of D30 and the side chain of S88. However, the interactions of NFV with D30 differ between

Table 4. Binding Free Energy of Each Model[a]

		ΔG_{int}^{ele}	ΔG_{int}^{vdw}	ΔG_{sol}	ΔG_b [b]	$\Delta\Delta G_b$ [c]	$\Delta\Delta G_b$ [d]
WT	B	−12.5 ± 1.4	−71.8 ± 3.8	15.1 ± 1.4	−69.2 ± 3.7		
Ref	AE	−12.8 ± 1.7	−70.8 ± 4.0	15.1 ± 1.5	−68.6 ± 3.7	0.6	
D30N	B	−6.9 ± 1.2	−70.5 ± 4.1	10.9 ± 0.9	−66.5 ± 3.9	2.7	
	AE	−7.5 ± 1.3	−70.2 ± 3.9	9.5 ± 1.0	−68.2 ± 3.7	1.0	0.4
N88S	B	−12.0 ± 1.3	−71.7 ± 3.8	15.0 ± 1.2	−68.7 ± 3.7	0.5	
	AE	−10.6 ± 1.4	−67.8 ± 4.0	12.8 ± 1.9	−65.6 ± 3.9	3.6	3.0

[a] Energy is presented in units of kcal/mol. [b] $T\Delta S$ is not included. [c] Difference from B(WT). [d] Difference from AE(Ref).

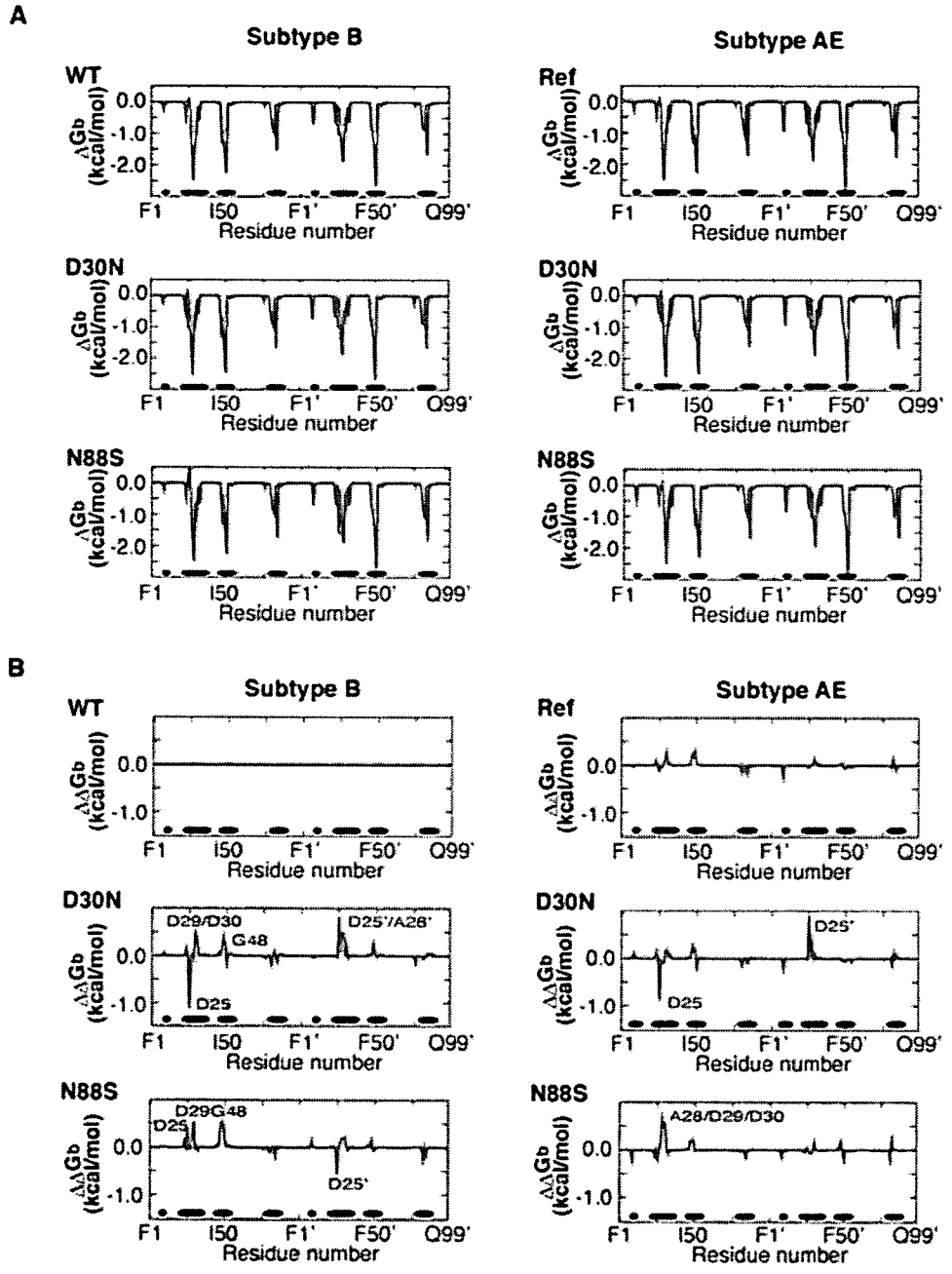

Figure 5. (A) Contribution of each individual residue to binding free energy. (B) Difference in contribution of each residue to the binding energy between the respective mutant and B(WT). The energies of contributions of the residues correspond to red solid lines, and those of B(WT) to green lines. The bottom black lines indicate the locations of the active site residues (R8, L23-V32, I47-I50, P81-I84, R8′, L23′-V32′, I47′-I50′, P81′-I84′).

subtype B and AE PRs. B(N88S) has a direct hydrogen bond between the main chain of D30 and NFV, whereas AE(N88S) mainly has one-water-molecule-mediated hydrogen bonds between the main chain of D30 and NFV. D30N PR has lower affinity with NFV than does N88S PR in subtype B HIV-1. In contrast, D30N PR has higher affinity than N88S PR in subtype AE HIV-1. These results are compatible with the results of a study by Ariyoshi et al.[16] Both D30N and N88S mutations in HIV-1 PRs exhibit significant losses of viral fitness.[20,21] Therefore, D30N and N88S mutants of HIV-1 have low growth kinetics relative to WT or Ref variants under the condition without any PIs. Nevertheless, it is frequently observed that the D30N mutant emerges in patients with subtype B HIV-1 in whom NFV treatment has failed and that the N88S mutant

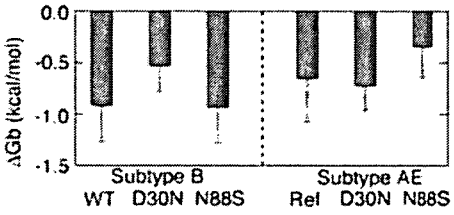

Figure 6. Contribution of the 30th residue to binding free energy in each model. Error bars stand for standard deviation.

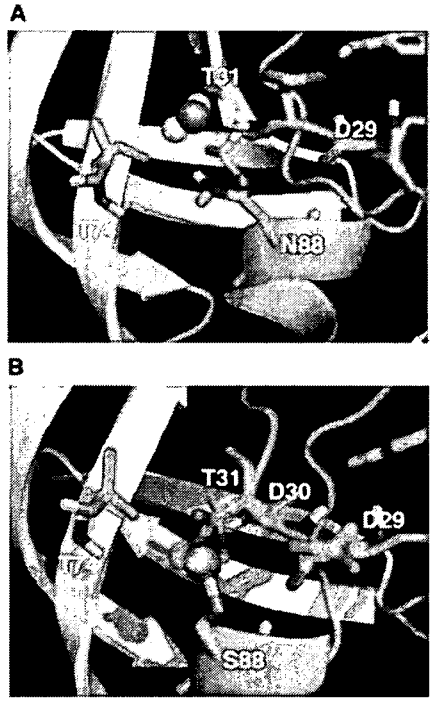

Figure 7. Hydrogen bond networks around the 88th residue of PR: (A) hydrogen bond networks in B(WT); (B) those in AE(N88S).

emerges in patients with subtype AE HIV-1.[16] These results indicate that the effectiveness of NFV is significantly reduced for these mutants. In contrast, N88S mutants of subtype B PR and D30N mutants of subtype AE PR have rarely been seen clinically. This is thought to be due not only to their low degree of fitness but also to their affinities with NFV comparable to those of subtype B WT or subtype AE Ref variants. Our simulations suggest that the natural polymorphisms of subtype AE PR, in spite of the nonactive site mutations, reduce the emergence rate of D30N and increase that of N88S.

The polymorphisms in subtype AE PR increase the emergence rate of N88S. However, there remains the question of which is the key mutation that affects the emergence rate of N88S among the polymorphisms K20R, E35D, M36I, R41K, H69K, L89M, and I93L. In this study, we focused on M36I for three reasons. First, M36I is related to the resistance against NFV.[46] Second, N88S has been observed in combination with mutations at various positions, including 20, 36, 46, 63, and 77.[19] Third, M36I is frequently observed as a polymorphism in other subtypes, namely, A and C.[13,14] We executed additional simulations of M36I PR, M36I/N88S PR, and L10F/M36I/N88S PR of subtype B HIV-1 in complex with NFV (labeled B(M36I), B(M36I/N88S), and B(L10F/M36I/N88S), respectively). L10F is a mutation that is frequently seen in CRF01_AE HIV-1 accompanied by N88S.[16] Our simulations suggest that the single M36I mutation in subtype B PR does not affect NFV binding. B(M36I) has stable hydrogen bonds between NFV and D30 (Supporting Information Table S3 and Figure S4). In contrast, the combination of M36I and N88S mutations in subtype B PR reduces the binding affinity with NFV. B(M36I/N88S) has fewer hydrogen bonds with NFV than does B(M36I) or B(N88S). Furthermore, the conformational change at D30 is larger in B(M36I/N88S) than in B(M36I) or B(N88S) (Supporting Information Figures S5 and S6). B(L10F/M36I/N88S) also creates fewer hydrogen bonds between NFV and D30 and causes conformational alteration at D30. The polymorphism M36I reduces the contribution of D30 to the binding with NFV (Supporting Information Figure S7). Our simulations suggest that N88S in subtype B PR reduces the binding affinity with NFV when it appears together with M36I.

It is interesting that both D30N and N88S confer resistance against NFV by decreasing the interaction between the 30th residue and NFV. Both D30N and N88S affect the active site residues around the 30th residue. Other active site residues hardly change their interaction with NFV or their conformations. As can be seen in Figure 2 and Figure S4, the NFV-resistant PRs (B(D30N), AE(N88S), B(M36I/N88S), and B(L10F/M36I/N88S)) each show an increase in distance between the 30th residue and NFV. The NFV-resistant N88S mutants (AE(N88S), B(M36I/N88S), and B(L10F/M36I/N88S)) each have a stable direct hydrogen bond between the side chain of S88 and the side chain of D30. Therefore, N88S does not appear simultaneously with D30N clinically.

Prior to the MD simulations, we reconsidered torsional force field parameters for the benzamide moiety in NFV. This moiety has essential hydrogen bonds with D30 of HIV-1 PR.[22,42] Thus, those torsional parameters are expected to greatly affect the results of the simulations. Nevertheless, the AMBER ff03[43] and general AMBER force fields[44] cause a much higher energy barrier around the rotatable bond between the benzene and amide groups in benzamide than that based on quantum chemical calculations (Supporting Information Figure S1). This was a serious problem for our simulations. Therefore, we improved the torsional force field parameters for the benzamide moiety in NFV by fitting them to the energy curve obtained from quantum chemical calculations. Our newly developed parameters enabled us to carry out precise simulations of HIV-1 PR in complex with NFV.

In this study, we not only proposed the mechanism of resistance against NFV of N88S in subtype AE PR but also examined the influence of the polymorphisms in subtype AE PR on the emergence rates of D30N and N88S mutations. N88S and the polymorphisms in subtype AE PR are all classified as nonactive site mutations. Nevertheless, these mutations affect the binding of NFV. We and other groups have reported that the nonactive site mutations affect the binding affinity of some inhibitors, the emergence rate of mutants, and the catalytic activity of the protease.[17,22,33,36,39,41,47–50] For example, the polymorphisms in subtype C HIV-1 enhance the catalytic efficacy. However, there have been few studies on the influence of nonactive site mutations from structural viewpoints. There have also been few studies on the differences between HIV-1 subtypes. Clarification of the roles of nonactive site mutations and polymorphisms will enable us to design potent drugs, since the currently available PIs were developed and tested only against subtype B PRs. Accumulation of data on the susceptibilities of nonsubtype B viruses to the currently available PIs is also needed in order to establish an effective HIV-1 therapy strategy. Clarification of these susceptibilities will also be useful for selecting more appropriate drugs for patients.